than an order of magnitude, a mean figure for the nighttime earth may be biased by the small sample and the degree of nonuniformity in Fig. 1.

About 200 storms (400 strokes) were detected in a time-area scan of 9500 deg^2 min. In other words, there appears to be one chance in 50 that in a given minute during the night there will be a thunderstorm complex in a 1-deg^2 area. Thunderstorm complexes are smaller than 1 deg^2 and in a given complex there are usually one or two electrically active cells producing an average of three flashes per minute (*1*). Brooks (*10*) as quoted by Humphreys (*11*), gives the average lifetime of a thunderstorm as about an hour. Thus the number of storms during the night between the above latitude limits is of the order of

$$\frac{25200 \text{ deg}^2 \times 720 \text{ min} \times 400 \text{ strokes}}{9500 \text{ deg}^2 \text{ min} \times 240 \text{ stroke/storm}} = \text{approx. } 3200$$

Although the storm frequency in general is higher during the day than during the night (*12*), the value obtained above is considerably lower than would have been expected from Brooks's figure of 44,000 storms per day. This discrepancy may be partly due to the threshold limit set for the satellite photometers and the difficulties of observing visual lightning output through the overlying cloud cover.

J. A. VORPAHL
Department of Physics, University of California, Berkeley 94720
J. G. SPARROW
E. P. NEY
School of Physics and Astronomy, University of Minnesota, Minneapolis

References and Notes

1. E. T. Pierce, paper given at Fourth International Conference on Universal Aspects of Atmospheric Electricity, Tokyo, 1968.
2. S. C. Coroniti, paper given at the International Astronautical Congress, Madrid, 1966.
3. G. S. Larson, R. J. Massa, S. C. Coroniti, paper given at Fourth International Conference on Universal Aspects of Atmospheric Electricity, Tokyo, 1968.
4. R. B. Bent, paper given at Fourth International Conference on Universal Aspects of Atmospheric Electricity, Tokyo, 1968.
5. J. A. Vorpahl, thesis, University of Minnesota (1967).
6. J. G. Sparrow, E. P. Ney, G. B. Burnett, J. W. Stoddart, *J. Geophys. Res.* **73**, 857 (1968).
7. J. G. Sparrow and E. P. Ney, *Science* **161**, 459 (1968).
8. S. I. Rasool, *J. Atmos. Sci.* **21**, 152 (1964).
9. A. Arking, in *Space Research* (North-Holland, Amsterdam, 1963), vol. 4, p. 133.
10. C. E. P. Brooks, *Geophys. Mem. London* **24** (1925).
11. W. J. Humphreys, *Physics of the Air* (McGraw-Hill, New York, 1929), chap. 17.
12. F. J. W. Whipple, *Quart. J. Roy. Meteorol. Soc.* **55**, 1 (1929).
13. We thank J. Stoddart for his work on the satellite and W. Elliott for programming the computer. This work was primarily supported under NASA contract NAS 5-3838. Substantial assistance was obtained under NASA contract NGL-24-005-008 and Office of Naval Research contract N00014-67-A-0113-0004.

24 June 1970

Deep-Sea Tides 1250 Kilometers off Baja California

Abstract. *The tidal pressure fluctuations on the sea floor were read by a sensitive optical sensor that detects the rotations of a multiturn Bourdon helix. The record was analyzed in terms of the transfer functions between tidal elevations and gravitational driving. Off California, the semidiurnal tide attenuates considerably faster than the diurnal tide. Neither species satisfies the rate of decay expected from a Kelvin wave.*

Very little is known about tides over the expanse of the open ocean mainly because the traditional method of measuring tidal fluctuations along the coast —that is, referring the sea level to a stationary structure—is not applicable over the open ocean. However, tidal pressure fluctuations on the sea floor can be measured and, since they reflect the mass variation of the water column, are in a sense more fundamental than tidal elevations.

Detection of 0.5-cm changes of waterhead over a 5-km depth requires an instrumental stability and resolution of 10^{-6}. Limiting the drift due to plastic flow of the transducers requires sensitive strain detectors. Vibrating wire transducers furnish adequate sensitivity (*1*) provided that the recorded data are corrected for temperature effects. My data were obtained with an instrument equipped with a ferronickel Bourdon tube transducer that discriminates between pressure and temperature effects (*2*). The necessary sensitivity is obtained by optical readout (*3*). I have previously shown (*2*) that the instrumental drift can be fully explained by Andrade's beta creep (*4*) of the pressurized Bourdon helix. Thus, when we apply these well-understood principles, a high degree of drift rejection is achieved.

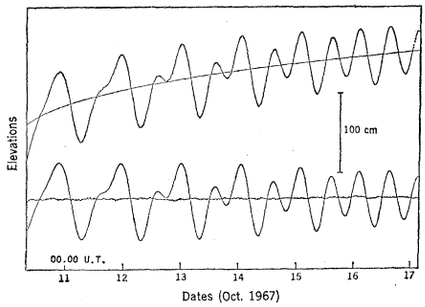

Fig. 1. The upper wavy line, slowly drifting upward, is a plot of the original data. The contribution of creep is superimposed on it, while the pure tidal and noise contributions are plotted below.

The observations were obtained during October 1968, 1150 km off Baja California, at a water depth of 4.4 km (24° 46.9′N, 129° 1.1′W). A plot of the original data is shown on Fig. 1 (upper wavy trace). Because of the extreme smoothness of the record, a simple least squares fit analysis with a series of harmonic functions permits resolution of many constituents in each species, a result not possible with equivalently short coastal records. We have also separated the diurnal constituents K_1 and P_1 and the semidiurnal constituents S_2 and K_2, taking into consideration their equilibrium amplitudes and phrases (see Table 1).

A more realistic method by which contamination of the resolved constituents by the unresolved ones can be avoided consists of estimating the transfer functions between gravitational forces and tidal response. Such an analysis has been carried out by a least squares fit technique in which the diurnal and semidiurnal transfer functions are computed separately to best advantage. The transfer functions are expanded in frequency-dependent Taylor series around the center of each tidal band. This yields a system of linear equations from which the coefficients of the successive terms are obtained. Analysis of the residual noise by a Fourier technique indicates how many terms in the Taylor expansion are required to bring the residual energy density in the tidal band below the adjacent level. With the record shown this result is achieved with the first two terms (Table 1). The Fourier spectra of the residual noise are shown for the harmonic method (Fig. 2a) and for the transfer function method with one and two terms (Fig. 2, b and c).

The errors in the calculated transfer functions are estimated by varying their parameters until the dips in the Fourier spectrum (Fig. 2c) at diurnal and semidiurnal frequencies disappear. When nongravitational and cusps energies (*5*)

Table 1. Constituent estimates and other pertinent comparative data. The error brackets are given for the modulus and phase of the transfer functions; SIO, Scripps Institution of Oceanography (La Jolla); AS, angular speed; A, amplitude.

Constituents	AS (deg/hr)	Harmonic method		Transfer function method: (two terms in Taylor expansion)			SIO observations		Dietrich phase (deg)	Bogdanov	
		A (cm)	Phase (deg)	A (cm)	Transfer function	Phase (deg)	A (cm)	Phase (deg)		A (cm)	Phase (deg)
K_1	15.04107	26.0	218	26.3	2.44 ± 0.15	221 ± 5	32.8	207	220	36.9	221
P_1	14.95893	8.7	217	8.5	2.39 ± 0.15	220 ± 5	10.6	192		11.1	220
O_1	13.94304	17.4	207	14.3	1.87 ± 0.23	201 ± 10	21.0	183	200	25.6	210
Q_1	13.39866	2.8	194	2.5	1.71 ± 0.28	187 ± 16	3.8	204		4.8	204
M_2	28.98410	21.2	103	22.4	1.11 ± 0.09	115 ± 8	48.9	143	62	34.7	172
S_2	30.00000	12.3	90	10.4	1.10 ± 0.11	97 ± 10	19.9	136	55	13.0	160
K_2	30.08214	3.4	90	2.8	1.10 ± 0.12	96 ± 11	5.6	131		4.5	159
N_2	28.43973	7.1	111	4.5	1.14 ± 0.10	124 ± 10	12.1	119		7.4	178
S_3	45.00000	0.3		0.2							
M_3	43.47616	0.1		0.2							
Residual noise amplitude		0.8 r.m.s.		1.2 r.m.s.							

are included in the amounts of 1.5 cm root mean square (r.m.s.) in each band, the upper limit of uncertainty in the transfer function is that seen in Table 1.

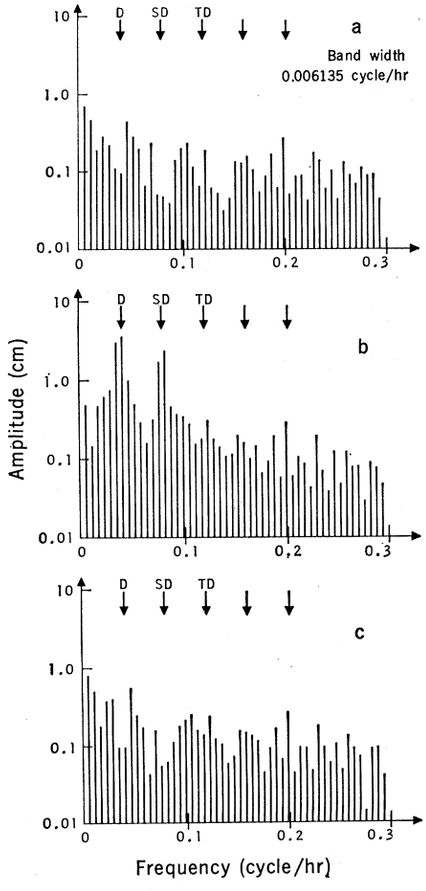

Fig. 2. Fourier analysis of the residual noise in the case of the harmonic analysis (a) of the transfer function technique with one term in the Taylor expansion (b) and two terms (c); *D*, diurnal; *SD*, semidiurnal; *TD*, tridiurnal.

Comparison of the results with Dietrich's cotidal maps (*6*) shows close agreement for the diurnal but not for the semidiurnal species (see Table 1). Observations and predictions can also be compared by the cotidal and corange maps for K_1, O_1, M_2, and S_2 computed by Bogdanov *et al.* (*7*). The predicted amplitudes are roughly 1.3 times larger than those observed for the diurnal and 1.5 times larger for the semidiurnal species (Table 1). Predicted and observed phases are consistent for the diurnal but not for the semidiurnal species. Because the solid earth is not infinitely rigid, it responds elastically to the gravitational potential of sun and moon. Furthermore, since the response involves only limited displacements, its lag behind the gravitational potential is negligible. The result is a reduction of the effective tide-driving potential. Available estimates of the appropriate Love numbers suggest a reduction from unity to approximately 0.65 (*8*). There seems to be little doubt that the amplitudes computed by Bogdanov *et al.* would be reduced appreciably if the tidal up-and-down motion of the sea floor were included in their calculations. By such methods, increased agreement between predictions and observations may be achieved.

The offshore decrease of amplitude revealed by observations of tides on islands suggests that tides are best modeled by Kelvin waves. These display an exponential decay of the form $\exp - (flx/\omega)$, where f is the Coriolis parameter, l is the wave number, ω is the angular speed, and x is the distance offshore. If coastal values from the Scripps Institution of Oceanography tide gauge in La Jolla (Table 1) are used, the amplitude ratios yield the values 0.81 for K_1 and 0.46 for M_2 compared to 0.70 predicted for both. The attenuation of the tide at the observation station is thus larger than that of a Kelvin wave for the diurnal and smaller for the semidiurnal tide, an observation which suggests that other modes of oscillation of the Pacific Basin must be involved. The absence of peaks in the Fourier spectrum at overtone frequencies of the tides (Fig. 2) indicates that both oceanic and instrumental responses are very linear. The noise distribution beyond the tidal bands is illustrated by the energy spectrum in Fig. 3. The noise energy falls sharply away from the tidal bands to a spectral density of 0.1 cm^2 $(cycle/hr)^{-1}$ at 0.5 cycle/hr and decreases regularly and slowly thereafter to a plateau with a density of 0.005 cm^2 $(cycle/hr)^{-1}$ around 35 cycle/hr. Meteorological effects and internal waves may account for an important part of the low-frequency background noise. To check whether an appreciable part of the noise at higher frequency could be associated

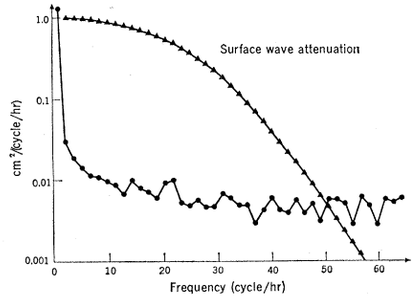

Fig. 3. Spectrum of the background noise (circles). The energy attenuation of surface waves at the ocean floor is indicated by triangles.

with long oceanic gravity waves, their quadratic attenuation at the bottom is also plotted on Fig. 3. The lack of similarity between the two curves indicates that no appreciable noise is contributed by surface waves in the band centered around 20 cycle/hr. The nature of the background noise in this area is uncertain. It could be explained by seismic fluctuations of the ocean floor, with a vertical amplitude of the order of 2×10^{-3} cm r.m.s. (20 μm) within the band, 10 to 30 cycle/hr acting against the 4.4-km water column. It may represent instrumental noise and may contain some noise due to higher-frequency signals such as those associated with microseisms.

JEAN FILLOUX
Gulf General Atomic Incorporated, San Diego, California 92112

References and Notes

1. S. D. Hicks, A. J. Goodheart, C. W. Iseley, *J. Geophys. Res.* **70**, 1827 (1965); M. Eyries, M. Dars, L. Eldely, *Cah. Oceanogr.* **9**, 1 (1964); F. E. Snodgrass, *Science* **162**, 78 (1968); A. A. Nowroozi, M. Ewing, J. E. Nafe, M. Flugel, *J. Geophys. Res.* **73**, 1921 (1968).
2. J. H. Filloux, *Trans. Int. Un. Geophys. Geodet.* (1969).
3. R. V. Jones and J. C. S. Richards, *J. Sci. Instr.* **36**, 90 (1959); J. H. Filloux, *Nature* **226**, 935 (1970).
4. E. N. Andrade, *Proc. Roy. Soc. London* **84**, 11 (1910); N. F. Mott, *Phil. Mag.* **44**, 742 (1953).
5. W. H. Munk and D. E. Cartwright, *Phil. Trans. Roy. Soc. London Ser. A* **259**, 533 (1966).
6. G. Dietrich, *General Oceanography, An Introduction* (Interscience, New York, 1963).
7. K. T. Bogdanov, K. V. Kim, V. A. Magarik, *Tr. Inst. Okeanol. Akad. Nauk SSSR* **75**, 73 (1964).
8. P. Melchior, *The Earth Tides* (Pergamon, Oxford, 1966).
9. I thank Drs. C. S. Cox, G. Groves, and R. L. Snyder for comments and suggestions. The opportunity of a Scripps Institution of Oceanography cruise to collect present data is appreciated.

19 March 1970; revised 22 May 1970

Composition Differences at Surfaces Detected by Adsorption and Desorption of Radiotracers

Abstract. *A novel method for the detection of composition differences on solid surfaces is based on differences in the adsorption and subsequent partial desorption of a radiotracer by heterogeneities of the surface.*

The detection of trace amounts of materials on surfaces is important in many applications in research work and industrial problems. Although there are a variety of methods such as radiotracer counting, measurements of contact angle, and ellipsometry by which one may detect trace residues and small differences in composition, each method has certain drawbacks and no one method is generally applicable. Thus there are many problems that would benefit from the application of a simple and sensitive method of broad applicability. We report here on such a method that makes possible the detection of subtle differences in composition at the surface of many solid materials such as glass, and the detection of adsorbed foreign materials on most solid surfaces.

Fig. 1. Autoradiograph of a thumbprint on a zinc borosilicate glass slide after adsorption of ^{14}C-labeled stearic acid from benzene solution and subsequent partial desorption with 1,1,2-trichlorotrifluoroethane. Industrial x-ray film was used with an exposure time of 120 hours.

In essence this method depends on the adsorption and subsequent partial desorption of radiotracers from solid surfaces, with autoradiography used as the means of detecting the distribution of adsorbed tagged material. The differences in adsorption and desorption arise from the inherently different adsorption/desorption characteristics of heterogeneities at the surface. An important feature of this method is that tagged compounds are used only to detect the differences in composition on the substrate of interest—the species constituting the surface itself need not be composed of tagged materials.

To illustrate the method, we describe its use to detect a thumbprint removed from a glass slide by means of a heat treatment and water rinse. A cover glass was cleaned by heating for 30 minutes in air at 450°C. A thumbprint was impressed on this cover glass [Corning No. 2935, a zinc borosilicate glass reported by Corning to have the following nominal composition (in percentage by weight): SiO_2, 62; Na_2O, 7; K_2O, 7; ZnO, 7; B_2O_3, 9; Al_2O_3, 2; TiO_2, 5; trace elements, 1], after which the slide was subjected to another 30-minute heat treatment at 450°C. At this point the thumbprint was still recognizable because of sodium chloride residues. After copious rinsing with distilled water, no traces of the thumbprint were visible to the naked eye, nor did examinations with ordinary light microscopy, transmission electron microscopy, scanning electron microscopy, and electron microprobe analysis reveal traces of the print. However, as the autoradiograph in Fig. 1 shows, the method described here did succeed in revealing the thumbprint after the heat treatment and rinsing procedure cited above. The thumbprint was made visible after the slide was immersed in a solution of ^{14}C-labeled stearic acid in benzene (2 mc/liter) for 26 hours and then was rinsed with 1,1,2-trichlorotrifluoroethane to remove excess stearic acid. The autoradiograph was made by exposing a sheet of industrial x-ray film (Cronex 506) to the slide for 120 hours.

We believe that in this particular case the heat treatment at 450°C caused enough ion exchange of Na^+ ions with other cations in the glass to bring about detectable differences in the adsorption/desorption characteristics of the substrate for stearic acid. Thus we have a method for detecting the rather subtle differences in cation surface densities in glass.

In other experiments in which semiconductor-grade silicon was used as the substrate ion exchange did not play a part in the process and adsorbed contaminants *on* the surface were detected rather than components in the surface. Other experiments in which gold and Mylar polyester film were used as substrates demonstrated that this technique is applicable to many substrates and contaminants. The wide choice of temperature, tagged adsorbent, time, and solvents available makes detection of a particular species feasible on virtually any solid substrate.

DALE A. BRANDRETH
RULON E. JOHNSON
Experimental Station, Organic Chemicals Department, E. I. du Pont de Nemours and Company, Wilmington, Delaware 19898

30 April 1970